

University of Groningen

## Antimicrobial peptides in action

Leontiadou, Hari; Mark, Alan E.; Marrink, Siewert J.

*Published in:*  
Journal of the American Chemical Society

*DOI:*  
[10.1021/ja062927q](https://doi.org/10.1021/ja062927q)

**IMPORTANT NOTE:** You are advised to consult the publisher's version (publisher's PDF) if you wish to cite from it. Please check the document version below.

*Document Version*  
Publisher's PDF, also known as Version of record

*Publication date:*  
2006

[Link to publication in University of Groningen/UMCG research database](#)

*Citation for published version (APA):*  
Leontiadou, H., Mark, A. E., & Marrink, S. J. (2006). Antimicrobial peptides in action. *Journal of the American Chemical Society*, 128(37), 12156-12161. <https://doi.org/10.1021/ja062927q>

### Copyright

Other than for strictly personal use, it is not permitted to download or to forward/distribute the text or part of it without the consent of the author(s) and/or copyright holder(s), unless the work is under an open content license (like Creative Commons).

The publication may also be distributed here under the terms of Article 25fa of the Dutch Copyright Act, indicated by the "Taverne" license. More information can be found on the University of Groningen website: <https://www.rug.nl/library/open-access/self-archiving-pure/taverne-amendment>.

### Take-down policy

If you believe that this document breaches copyright please contact us providing details, and we will remove access to the work immediately and investigate your claim.

*Downloaded from the University of Groningen/UMCG research database (Pure): <http://www.rug.nl/research/portal>. For technical reasons the number of authors shown on this cover page is limited to 10 maximum.*

## Antimicrobial Peptides in Action

Hari Leontiadou,<sup>†</sup> Alan E. Mark,<sup>‡</sup> and Siewert J. Marrink<sup>\*,†</sup>

*Contribution from the Department of Biophysical Chemistry, Biomolecular Sciences and Biotechnology Institute, University of Groningen, Nijenborgh 4, 9747 AG Groningen, The Netherlands, and School of Molecular and Microbial Science, University of Queensland, St. Lucia, Brisbane, QLD 4072, Australia*

Received April 27, 2006; E-mail: s.j.marrink@rug.nl

**Abstract:** Molecular dynamics simulations of the magainin MG-H2 peptide interacting with a model phospholipid membrane have been used to investigate the mechanism by which antimicrobial peptides act. Multiple copies of the peptide were randomly placed in solution close to the membrane. The peptide readily bound to the membrane, and above a certain concentration, the peptide was observed to cooperatively induce the formation of a nanometer-sized, toroidally shaped pore in the bilayer. In sharp contrast with the commonly accepted model of a toroidal pore, only one peptide was typically found near the center of the pore. The remaining peptides lay close to the edge of the pore, maintaining a predominantly parallel orientation with respect to the membrane.

### Introduction

Magainins are peptides found in the skin of the African clawed frog *Xenopus laevis*<sup>1</sup> that exhibit a wide range of antimicrobial and antifungal activity. They are cationic and amphipathic peptides that bind to the membrane surface, adopting a predominantly  $\alpha$ -helical structure.<sup>2,3</sup> At high concentrations they permeabilize the lipid matrix,<sup>4,5</sup> forming water-filled, nanometer-sized pores<sup>6</sup> that lead to cell death. Experimentally, it is observed that as the concentration of bound peptide is increased past the permeabilization threshold there is a change in the orientation from the peptides being essentially parallel<sup>7,8</sup> to at least a proportion of the peptides having a perpendicular orientation.<sup>4</sup> This is associated with an increase in lipid flip-flops and the translocation of peptide across the membrane.<sup>5</sup> On the basis of these findings, it is commonly accepted that magainins (as well as many other antimicrobial peptides) form toroidal pores.<sup>4,5,9</sup> The main characteristic of a toroidal pore is that it is hydrophilic. The peptides are believed to stabilize the pore by interacting strongly with the lipid headgroups that line the pore. In fact, despite being very intensively studied experimentally, relatively little is known

regarding the mechanism of pore formation or the structure of the pore itself.

Here, we present the results of atomistic molecular dynamics (MD) simulations of magainin peptide interacting with a dipalmitoylphosphatidylcholine (DPPC) phospholipid bilayer. The specific peptide used in this study is the 23 amino acid (aa) MG-H2 peptide, an analogue of the well-studied antimicrobial peptide magainin-2 (MG-2).<sup>10</sup> MG-H2 (IIKKF-LHSIWKF GKAFVGEIMNI) is positively charged (+3) at physiological pH (see Figure 1) and was chosen for this study as unlike other members of the magainin family MG-H2 has a high affinity for neutral phospholipids such as DPPC. Besides the advantage that MG-H2 can be used in combination with the well-modeled lipid DPPC, it forms pores more easily than the parent magainin. This is attributed to its higher hydrophobic moment.<sup>10</sup> Note that the charge–charge interactions between the peptide and the anionic lipids are not directly involved in pore formation; it is hypothesized that they only provide the long-range attraction needed to bring the peptides close to the surface.<sup>11</sup>

### Methods

**Setup.** The systems simulated contained 1, 2, or 4 MG-H2 peptides, 128 DPPC lipids, and 6000 water molecules. The corresponding peptide/lipid (P/L) ratios are 1/128, 2/128, or 4/128. Multiple simulations were performed for each system, starting from different initial random velocity distributions. Initially, the peptides are in an  $\alpha$ -helical configuration and are solvated in the water phase close to one of the monolayers of an equilibrated bilayer (see Figure 1). The asymmetric distribution of the peptides mimics the addition of peptide to a solution containing cells or liposomes, in which peptides adsorb to one

<sup>†</sup> University of Groningen.

<sup>‡</sup> University of Queensland.

- (1) Zasloff, M. *Proc. Natl. Acad. Sci. U.S.A.* **1987**, *84*, 5449–5453.
- (2) Marion, D.; Zasloff, M.; Bax, A. *FEBS Lett.* **1988**, *227*, 21–26.
- (3) Chen, H. C.; Brown, J. H.; Morell, J. L.; Huang, C. M. *FEBS Lett.* **1988**, *236*, 462–466.
- (4) Ludtke, S. J.; He, K.; Heller, W. T.; Harroun, T. A.; Yang, L.; Huang, H. W. *Biochemistry* **1996**, *35*, 13723–13728.
- (5) Matsuzaki, K.; Murase, O.; Fujii, N.; Miyajima, K. *Biochemistry* **1996**, *35*, 11361–11368.
- (6) He, K.; Ludtke, S.; Huang, H. W.; Worcester, D. L. *Biochemistry* **1995**, *34*, 5614–5618.
- (7) Ludtke, S. J.; He, K.; Wu, Y.; Huang, H. W. *Biochim. Biophys. Acta* **1994**, *1190*, 181–184.
- (8) Matsuzaki, K.; Murase, O.; Tokuda, H.; Funakoshi, S.; Fujii, N.; Miyajima, K. *Biochemistry* **1994**, *33*, 3342–3349.
- (9) Epand, R. M.; Vogel, H. J. *Biochim. Biophys. Acta* **1999**, *1462*, 11–28.

(10) Tachi, T.; Epand, R. F.; Epand, R. M.; Matsuzaki, K. *Biochemistry* **2002**, *41*, 10723–10731.

(11) Hallock, K. J.; Lee, D. K.; Ramamoorthy, A. *Biophys. J.* **2003**, *84*, 3052–3060.

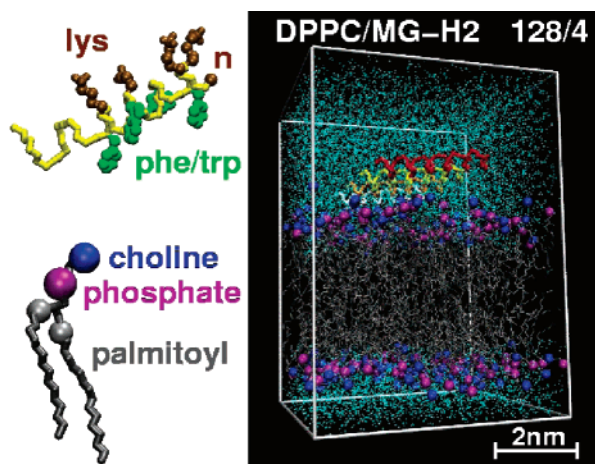


**Figure 1.** Snapshot of the starting configuration of a system containing 4 magainin (MG-H2) peptides and 128 lipid (DPPC) molecules. The lipid headgroups are represented as blue (choline) and purple (phosphate) spheres. The lipid tails are gray, and water is blue. The backbones of the different peptides are shown in yellow, orange, red, and white. The image to the left shows key functional side chains in green (hydrophobic residues) or brown (charged lysines and N-terminal).

**Table 1.** Overview of Simulations Performed<sup>a</sup>

label	no. of peptides	conditions	aggregation state	simulation time (ns)	pore formation time (ns)
A1	1	stress-free	monomeric	80	
A2	2	stress-free	monomeric	113	
B2	2	stress-free	monomeric	64	
C2	2	stressed	monomeric	121	
D2	2	stressed	cluster	134	
E2	2	stressed	cluster	152	
F2	2	stressed	cluster	88	44
A4	4	stress-free	partly clustered	80	
B4	4	stress-free	cluster	250	35
C4	4	stress-free	cluster	20	17
D4	4	stress-free	cluster	122	63
E4	4	stress-free	cluster	250	55
F4	4	stressed	partly clustered	60	
G4	4	stressed	cluster	193	
H4	4	stressed	cluster	220	107
R1	1	random		60	unstable
R2	2	random		134	unstable
R3	3	random		144	stable

<sup>a</sup> The number of peptides in the system is varied between 1 and 4. Simulations were performed at either stress-free ( $\gamma = 0$  mN/m) or stressed ( $\gamma = 20$  mN/m) conditions. The total simulation time is indicated, plus the time required for a pore to form. The aggregation state of the peptides on the surface at the time of pore formation or at the end of the simulation when no pore was formed is indicated as monomeric for peptides that do not strongly interact or clustered if all peptides are aggregated together. Partly clustered denotes that only two out of four peptides aggregated. A few simulations were performed starting from a random mixture of the components. During the spontaneous aggregation of lipids into a bilayer, a pore always forms as a metastable intermediate.<sup>22</sup> Only in the case of three peptides the pore remained stable throughout the simulation.

monolayer only. To test whether the pores obtained were fully equilibrated, three additional simulations were performed starting from a random distribution of lipids, peptides, and water at P/L = 1/128, 2/128, and 3/128. An overview of the simulations performed is given in Table 1. Most systems were run between 20 and 100 ns, depending on when, and if, a pore was actually formed. Two simulations were extended to 250 ns to study the long-time behavior of the pore.

**Simulation Parameters.** The GROMACS software package<sup>12</sup> was used to perform all the MD simulations. The force field for DPPC was

taken from a previous study (setup E<sup>13</sup>). The GROMOS force field 43a2<sup>14</sup> was used to describe the peptide interactions. Both force fields were parametrized for use with a group-based twin range cutoff scheme (using cutoffs of 1.0/1.4 nm and a pairlist update frequency of once per 10 steps) including a reaction field correction<sup>15</sup> with  $\epsilon = 78$  to account for long-range electrostatic interactions. The water was modeled as SPC.<sup>16</sup> A time step of 2 fs was used. Bond lengths were constrained using the LINCS algorithm.<sup>17</sup> The simulations were performed in the  $NP_{\parallel}P_zT$  ensemble using periodic boundary conditions. The temperature was weakly coupled<sup>18</sup> (coupling time 0.1 ps) to  $T = 323$  K, above the main-phase transition temperature of DPPC. The pressure was also weakly coupled<sup>18</sup> (coupling time 0.5 ps, compressibility  $5 \times 10^{-5}$  bar<sup>-1</sup>) using a semiisotropic coupling scheme in which the lateral ( $P_{\parallel}$ ) and perpendicular ( $P_z$ ) pressures are coupled independently. Two sets of simulations were performed, one in which both  $P_{\parallel} = P_z = 1$  bar, resulting in a bilayer under stress-free conditions ( $\gamma = 0$ ), and another set using  $P_{\parallel} = -30$  and  $P_z = 1$  bar, which correspond to a bilayer under a lateral tension of 20 mN/m. Although the first set more realistically models the stress-free conditions in typical experimental setups, the second set was (wrongly) anticipated to speed up the pore formation process. See Table 1 for an overview of the conditions used in each of the simulations performed. Note that a tension of 20 mN/m is actually larger than a phospholipid membrane would be able to withstand in an experimental situation. Rupture typically occurs around a few millinewtons per meter.<sup>19,20</sup> However, pore formation preceding membrane rupture is a kinetic process and therefore depends on the loading rate of the applied tension.<sup>20</sup> In MD simulations the effective loading rate is high enough to prevent pore formation in pure DPPC membranes up to tensions of  $\sim 90$  mN/m.<sup>21</sup>

**Analysis.** The lipid bilayer was characterized by analysis of the membrane thickness, interfacial width, and lipid tail order parameters. The thickness was defined as the average phosphate–phosphate distance. The interfacial width was measured by the standard deviation of the phosphate distribution. Lipid tail order parameters were computed with respect to the membrane normal axis.<sup>23</sup> The size of the pore was estimated from the diameter of a circle fitted to the glycerol/water interface of the pore (see Figure 4, lower panel). Taking the limits of the pore to be the region lying between the two planes corresponding to the glycerol/water interfaces, the average number of water molecules and lipid headgroups in the pore could be estimated. The permeation rate of water through the pores was estimated by counting the amount of water molecules that crossed both of the interfacial planes during the simulation. Lipid flip-flops were monitored by crossing of the bilayer midplane of the phosphate moiety of the lipid headgroup. The helicity of the peptides was determined using the DSSP criteria.<sup>24</sup> The

(12) Lindahl, E.; Hess, B.; van der Spoel, D. *J. Mol. Model.* **2001**, 7, 306–317.

- (13) Anézo, C.; de Vries, A. H.; Höltje, H. D.; Tieleman, D. P.; Marrink, S. J. *J. Phys. Chem. B* **2003**, 107, 9424–9433.  
 (14) van Gunsteren, W. F.; Krüger, P.; Billeter, S. R.; Mark, A. E.; Eising, A. A.; Scott, W. R. P.; Hünenberger, P. H.; Tironi, I. G. *Biomolecular Simulation: The GROMOS96 Manual and User Guide*; Biomos/Hochschulverlag AG an der ETH Zürich: Groningen/Zürich, 1996.  
 (15) Tironi, I. G.; Sperb, R.; Smith, P. E.; van Gunsteren, W. F. *J. Chem. Phys.* **1995**, 102, 5451–5459.  
 (16) Berendsen, H. J. C.; Postma, J. P. M.; van Gunsteren, W. F.; Hermans, J. Interaction models for water in relation to protein hydration. In *Intermolecular Forces*; Pullman, B., Ed.; Reidel: Dordrecht, The Netherlands, 1981; pp 331–342.  
 (17) Hess, B.; Bekker, H.; Berendsen, H. J. C.; Fraaije, J. G. E. M. *J. Comput. Chem.* **1997**, 18, 1463–1472.  
 (18) Berendsen, H. J. C.; Postma, J. P. M.; van Gunsteren, W. F.; DiNola, A.; Haak, J. R. *J. Chem. Phys.* **1984**, 81, 3684–3689.  
 (19) Zhelev, D. V.; Needham, D. *Biochim. Biophys. Acta* **1993**, 1147, 89–104.  
 (20) Evans, E.; Heinrich, V. *Compte Rendus* **2003**, 4, 265–274.  
 (21) Leontiadou, H.; Mark, A. E.; Marrink, S. J. *Biophys. J.* **2004**, 86, 2156–2164.  
 (22) Marrink, S. J.; Lindahl, E.; Edholm, O.; Mark, A. E. *J. Am. Chem. Soc.* **2001**, 123, 8638–8639.  
 (23) Egberts, E.; Marrink, S. J.; Berendsen, H. J. C. *Eur. Biophys. J.* **1994**, 22, 423–426.  
 (24) Kabsch, W.; Sander, C. *Biopolymers* **1983**, 22, 2577–2637.



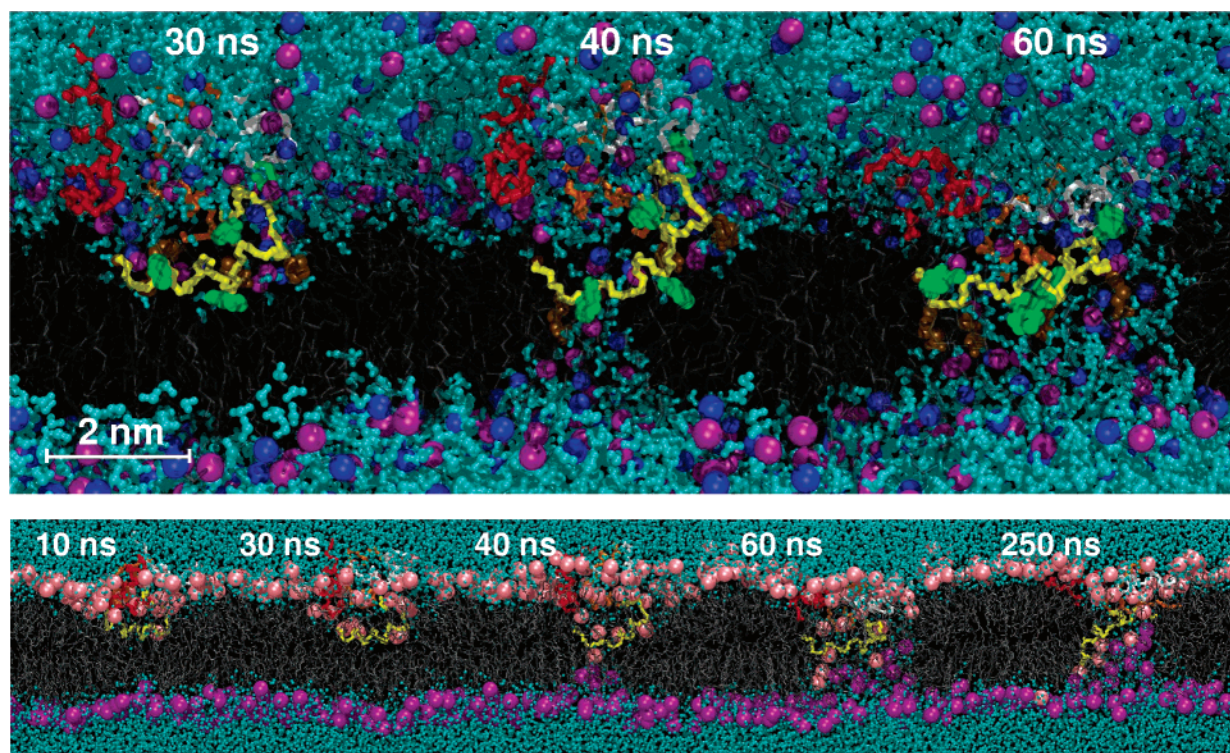


**Figure 2.** Antimicrobial action in atomic detail: Snapshots from a simulation showing the spontaneous formation of a pore in a DPPC lipid bilayer by the antimicrobial magainin peptide MG-H2. The peptide/lipid ratio was  $P/L = 4/128 = 1/32$ . Initially placed in the aqueous phase ( $t = 0$  ns; see Figure 1), the peptides aggregate during binding to the membrane interface ( $t = 10$  ns). After binding, one peptide moves toward the bilayer interior ( $t = 30$  ns). This induces stress in the membrane, resulting in the sudden formation of a pore ( $t = 40$  ns). The pore rapidly adopts a toroidal shape. One peptide can be seen penetrating through the membrane; the other peptides line the mouth of the pore ( $t = 60$  ns). This structure remains stable for the remainder of the simulation ( $t = 250$  ns). The backbones of the different peptides are shown in yellow, orange, red, and white. Key functional side chains are highlighted (upper panel). The lipid tails are gray, and water is cyan. The headgroups are represented as blue (choline) and purple (phosphate) spheres in the upper panel or as pink/purple spheres (phosphate) in the lower panel depending on whether the group was initially located in the monolayer to which the peptides bound.

aggregation of peptides on the bilayer interface was monitored by visual inspection. All visual analysis and graphical images were made using VMD.<sup>25</sup>

## Results and Discussion

**Antimicrobial Peptides in Action.** Figure 2 shows a series of snapshots from a simulation (B4) in which four copies of the magainin MG-H2 peptide spontaneously induce the formation of a stable transmembrane water pore. Initially placed randomly in solution close to the surface of the membrane, the peptides rapidly (within 10 ns) bind to the lipid interface. Upon binding to the membrane, the peptides aggregate and orient such that the hydrophobic side chains of the peptide, in particular the phenylalanine and the tryptophan side chains, interact with the interior of the membrane. Shortly after binding to the membrane, one of the peptides begins to embed deep into the interface (snapshot at  $t = 30$  ns). This appears to be a cooperative process resulting from the interaction of the overlying peptides with the lipid headgroups. Although the peptide is embedded quite deeply within the membrane, the charged lysine residues remain hydrogen bonded with the glycerol and phosphate moieties of the lipid headgroups. The system is metastable in this state for  $\sim 10$  ns until a fluctuation in the membrane/water interface leads to solvent molecules from the peptide-free interface interacting with hydrophilic groups of the embedded peptide. Once solvent molecules make contact

with the peptide, a contiguous pore opens rapidly (within a few nanoseconds). During this process, the peptide together with some lipid molecules moves across the membrane (snapshots at  $t = 40$  and 60 ns). The final stage of the process involves the relaxation of the pore toward a toroidal shape ( $t = 250$  ns).

This basic sequence of events (i.e., the initial embedding of a single peptide deep within the bilayer and increased structural fluctuations leading to translocation and relaxation to a toroidal pore) was observed in six independent simulations (see Table 1). The time required for pore formation varied between 10 and 100 ns, indicating that it is a stochastic event. Although the statistics obtained from the set of simulations are limited, spontaneous pore formation appears to be favored by two conditions: (i) a critical concentration is required, and (ii) the peptides need to be aggregated.

**Pore Formation is Concentration Dependent.** The first condition is apparently met for systems containing more than two copies of the peptide. When only one or two peptides are placed in the simulation box, the peptides bind to the interface but, except for one case, do not induce pore formation. Experimentally, magainin peptides only induce pore formation above a specific threshold concentration,  $1/100 < P/L < 1/30$ .<sup>4,7,26,27</sup> While this is similar to the concentration at which pore formation was observed in the simulations ( $P/L = 1/32$ ), a direct comparison is not possible, as we cannot rule out the

(25) Humphrey, W. Dalke, A.; Schulten, K. *J. Mol. Graphics* **1996**, *14*, 33–38.

(26) Dempsey, C. L.; Ueno, S.; Avison, M. B. *Biochemistry* **2003**, *42*, 402–409.

(27) Bechinger, B. *Biochim. Biophys. Acta* **1999**, *1462*, 157–183.

possibility that pores form on time scales beyond those accessible in the simulations. The absence of pore formation on the time scale of the simulations is not proof that interfacially adsorbed peptides are the true equilibrium state at low concentrations. The system might be kinetically trapped. Besides, in the macroscopic system local fluctuations in concentration exist which are absent in the microscopic simulation box. Nevertheless, pore formation in the simulations, like in experiments, requires a certain threshold concentration. One mechanism of pore formation which would give rise to a threshold concentration and for which there is some theoretical justification<sup>28,29</sup> is based on the proposition that the adsorption of peptide induces tension within the membrane which is relieved by pore formation. According to this model, only when the membrane tension reaches a critical value (corresponding to the threshold peptide concentration) is the opposing line tension overcome. At this point pore formation becomes favorable.

Our results indicate that the binding of the peptide to the membrane creates a local tension. The tension being induced is, however, asymmetric and differs in nature between the two monolayers. The tension, or stress, experienced in the monolayer to which the peptides are binding is of compressive nature. The excluded volume of the peptides forces the lipids to be squeezed more tightly together. Due to the intrinsic coupling between the two leaflets, the tension experienced by the other, peptide-free, monolayer is of opposite nature; i.e., the lipid area increases beyond the equilibrium area. The maximum expansion in area is observed in the simulations where four peptides bind. The area expands from 0.655 nm<sup>2</sup> for the pure membrane to 0.675 nm<sup>2</sup> when the peptides are fully bound but a pore has not yet formed. Comparison to previous simulations in which the effect of external stress on DPPC bilayers was studied reveals that an area expansion of ~3% is also obtained when an external tension of ~15 mN/m is applied.<sup>21</sup> The expansive stress on the peptide-free monolayer is thus on this order. Under stress-free external conditions ( $\gamma = 0$ ), the stress in the monolayer to which the peptides bind will be of the same magnitude but of compressive nature. Simulations were performed also at  $\gamma = 20$  mN/m (see Table 1). Application of external stress does not seem to enhance pore formation, implying that it is the difference in stress created between the monolayers upon peptide binding that is important. This might explain why pore formation has not been observed in previous MD simulations of antimicrobial peptide binding which have focused on isolated peptides and/or a symmetric distribution of the peptide on both sides of the bilayer.<sup>30–32</sup> Note that the effective tension of 15 mN/m experienced by the peptide-free monolayer is already larger than the experimental rupture limit of phospholipid membranes.<sup>19,20</sup> The straightforward conclusion stating that the geometric effect of peptide binding alone is sufficient to explain the action of the peptides is an oversimplification, however. On the time scales employed by the simulations, membranes can withstand much higher tensions (up to 90 mN/m<sup>21</sup>) due to energy barriers involved in pore formation.<sup>20</sup> The observation that pore formation in the

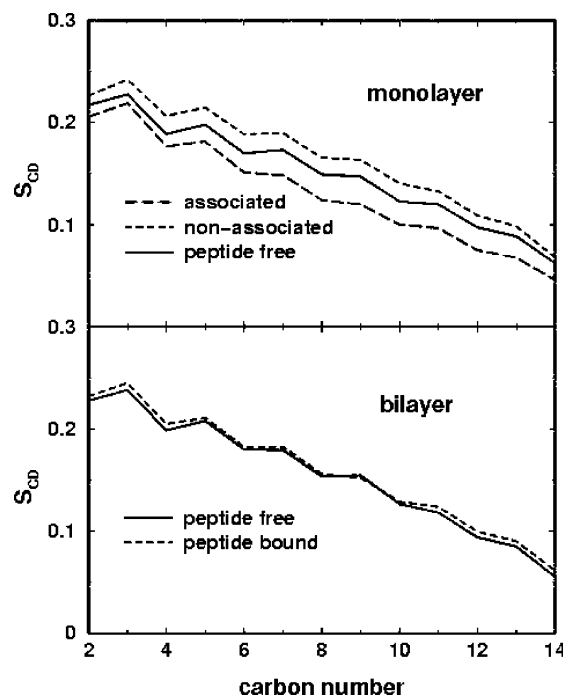


**Figure 3.** Lipid tail order parameters of the Sn1 chain obtained from a simulation with two peptides bound to the interface (A2). The upper panel distinguishes between lipids in the peptide-free monolayer and in the monolayer to which the peptides bind, divided between peptide-associated and nonassociated lipids. The lower panel compares the averaged order parameter profile for all lipids with and without peptides bound.

presence of the peptides occurs at a much lower effective tension thus points to a specific role of the peptides themselves.

**Peptide Aggregation Favors Pore Formation.** Our simulations further indicate that an aggregate involving multiple peptides promotes pore formation. Clustering occurred sometimes during binding to the interface, as indicated in Table 1. In all cases where pore formation was observed, the peptides were clustered together. There is some controversy in the literature regarding whether the direct interaction between peptides as observed in the simulations is required for pore formation. Certainly, experimental measurements suggest peptide aggregation is favorable. For example, a dimerized magainin analogue<sup>26</sup> shows enhanced activity. Nevertheless, theoretical arguments both in favor of aggregation<sup>29</sup> and against it<sup>33</sup> have been proposed. Aggregation would favor the hypothesis that pore formation by charged peptides is essentially similar to electroporation.<sup>34,35</sup> Accordingly, the strong local electrostatic field induced by an aggregated cluster of peptides suffices to trigger pore formation. The importance of the charged residues is further implicated by preliminary results which show that pore formation is less favorable at increased salt concentrations. Our simulations are insufficient to determine whether aggregation is essential. Nevertheless, our results indicate that aggregation at the interface enhances pore formation. On the basis of the two observations that (i) a threshold concentration is required to create enough stress in the membrane and (ii) pore formation is facilitated by aggregation of the peptides on the membrane interface, we conclude that pore formation, at least for the magainin analogue studied here, is a cooperative process.

(28) Huang, H. W.; Chen, F. Y.; Lee, M. T. *Phys. Rev. Lett.* **2004**, *92*, 198304.

(29) Zemel, A.; Ben-Shaul, A.; May, S. *Eur. Biophys. J.* **2005**, *34*, 230–242.

(30) Shepherd, C. M.; Vogel, H. J.; Tieleman, D. P. *Biochem. J.* **2003**, *370*, 233–243.

(31) Kandasamy, S.; Larson, R. G. *Chem. Phys. Lett.* **2004**, *132*, 113–132.

(32) Appelt, C.; Eisenmenger, F.; Kühn, R.; Schmieder, P.; Söderhäll, J. A. *Biophys. J.* **2005**, *89*, 2296–2306.

(33) Huang, H. W. *Biochemistry* **2000**, *39*, 8347–8352.

(34) Miteva, M.; Andersson, M.; Karshikoff, A.; Ottig, G. *FEBS Lett.* **1999**, *462*, 155–158.

(35) Gurtovenko, A. A.; Vattulainen, I. *J. Am. Chem. Soc.* **2005**, *127*, 17570–17571.



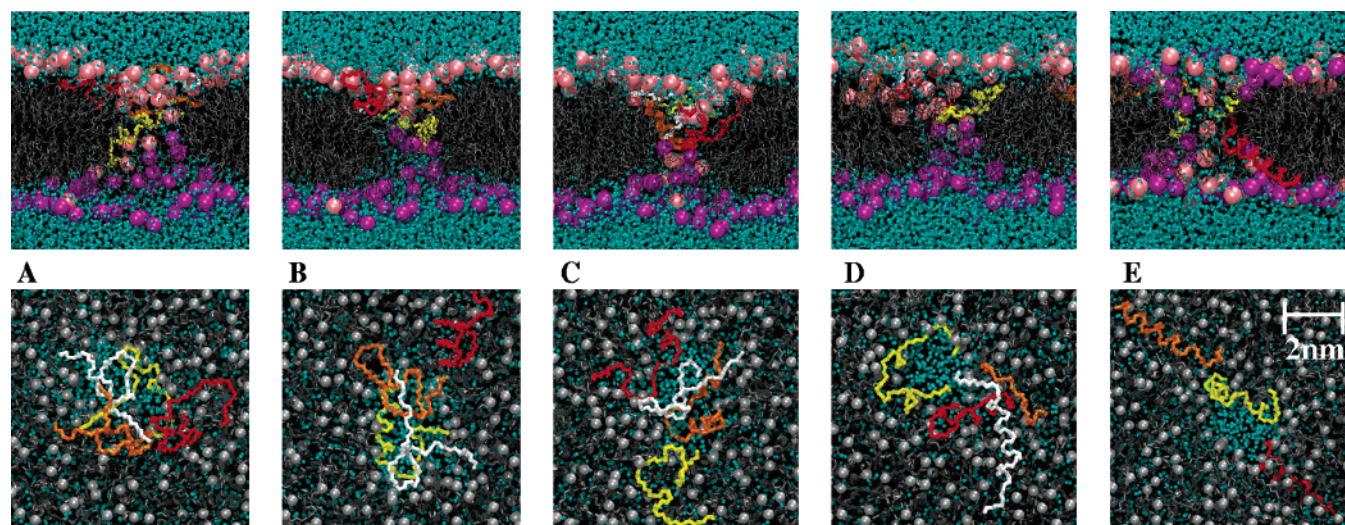


**Figure 4.** Diversity of toroidal pore structures formed by magainin peptides. Shown are the final structures of five independent simulations: (A–C) pores formed under stress-free external conditions, (D) pore formed in a bilayer at  $\gamma = 20$  mN/m, (E) pore formed by the aggregation of an initially random mixture of water, lipid, and peptide. Color code: The backbones of the peptides are shown in yellow, orange, red, and white. Lipid tails are gray. The phosphate atoms of the headgroups are pink spheres or purple depending on whether they initially resided in the monolayer to which the peptides adsorbed. The upper panel shows cross-sections through the bilayer. The lower panel shows a top view. The water above the bilayer and the lipid headgroups have been removed for clarity. The gray spheres represent the glycerol moieties.

#### Bilayer Order Changes Asymmetrically upon Peptide Binding.

The differential effect of peptide binding on the two monolayers is also reflected in asymmetric perturbation of lipid order. This is illustrated in Figure 3, which shows the order parameter profile for lipid tails in the peptide-free monolayer and in the peptide-binding monolayer. In the latter case a distinction is made between lipids in direct contact with the peptides and lipids not in direct contact. In comparison to that of the peptide-free bilayer, the lipid order is increased for the lipids that are in the peptide-bound monolayer when not in direct contact with the peptides. For the lipids adjacent to the peptides the order is decreased. In the peptide-free monolayer the lipid tails are also more disordered in comparison with those in a peptide-free bilayer. Averaged over the two monolayers, the total order of the lipids does not change significantly. The thickness of the bilayer also shows no apparent shift on peptide binding in our simulations. The phosphate–phosphate distance remains at  $0.375 \pm 0.005$ . Experimentally, both disordering<sup>36</sup> and ordering<sup>37</sup> of lipid tails in the presence of magainin have been measured. A small decrease in thickness, between 0.1 and 0.2 nm, has been reported.<sup>38</sup> Previous MD simulations report mixed observations<sup>30–32</sup> with respect to both lipid order and bilayer thickness. It therefore appears that the effect of peptide binding on the structural properties of bilayers is subtle and system dependent. The clear difference in order between the two monolayers is in line with recent simulation results.<sup>39</sup> A concomitant result of the local stress experienced by the peptide-free monolayer is an increase in structural fluctuations within the water–lipid interface. Such fluctuations of the interface are reflected in, for example, the width of the phosphate distribution of the peptide-free monolayer, which increases from 0.33 to 0.47 nm in the case of four peptides binding. The enhanced

fluctuations facilitate the formation of the pore. Once the pore forms, the stress difference is rapidly released.

#### Peptide Conformation and Orientation Show a Large Spread.

Another aspect which is apparent from the simulations is that the peptides are not highly structured and that a helical conformation is not required for pore formation. The peptides were initially placed in solution in a helical conformation. Unfolding takes place while the peptides are still in the aqueous phase. CD measurements suggest that magainin peptides are not structured in solution,<sup>40</sup> whereas bound to PC bilayers MG-H2 is approximately 50%  $\alpha$ -helical.<sup>10</sup> In the simulations the average helicity is somewhat lower (15–50%), although it is not possible to make a direct quantitative comparison between the two measures. It also cannot be ruled out that the refolding takes place over longer time scales. However, it is clear from our results that  $\alpha$ -helicity is not a prerequisite for pore formation. In fact, as experimental studies involving stabilized  $\alpha$ -helical peptides have shown reduced antimicrobial activity,<sup>41</sup> partial unfolding might facilitate pore formation. Note that the amphipathicity is retained even when MG-H2 is largely unfolded.

Figure 4 shows the final equilibrated structure of pores obtained from four independent simulations of peptide-induced pore formation (B4, D4, E4, H4), plus an additional pore obtained through spontaneous aggregation of the components starting from a random distribution (R3). In all cases the pores are toroidal in shape, with an internal diameter of  $2 \pm 0.5$  nm, and  $3 \pm 1$  nm at the rim. The size of the pores observed in the simulations closely matches the estimated size of 2–3 nm on the basis of experimental measurements.<sup>4</sup> The pores contain on average  $7 \pm 1$  headgroups and  $90 \pm 10$  water molecules. In no simulation do we find an arrangement of peptides that is similar to that proposed in commonly accepted models of a toroidal pore<sup>4,5</sup> in which multiple peptides line the central water channel in a perpendicular orientation. In contrast, only one or two

(36) Münster, C.; Spaar, A.; Bechinger, B.; Salditt, T. *Biochim. Biophys. Acta* **2002**, *1562*, 37–44.

(37) Boggs, J. M.; Jo, E.; Polozov, I. V.; Epand, R. F.; Anantharamaiah, G. M.; Blazyk, J.; Epand, R. M. *Biochim. Biophys. Acta* **2001**, *1511*, 28–41.

(38) Ludtke, S. J.; He, K.; Huang, H. W. *Biochemistry* **1995**, *34*, 16764–16769.

(39) Kandasamy, S.; Larson, R. G. *Biochim. Biophys. Acta*, in press.

(40) Bechinger, B. *Crit. Rev. Plant. Sci.* **2004**, *23*, 271–292.

(41) Houston, M. E.; Kondejewski, L. H.; Karunaratne, D. N.; Gough, M.; Fidai, S.; Hodges, R. S.; Hancock, R. E. W. *J. Pept. Res.* **1998**, *52*, 81–88.

peptides are located near the center of the pore. The other peptides remain bound at the surface of the membrane close to the mouth of the pore. In addition, there is considerable variation in the orientation of the peptides with respect to the membrane surface. The orientation of the peptides is in general close to parallel. The average angle of the peptide backbone with respect to the membrane surface is  $25^\circ$  with a standard deviation of  $20^\circ$ . The primary difference between the pores formed by the spontaneous aggregation of all components and pores formed by the addition of peptide to a preformed bilayer is the distribution of the peptide. Random aggregation results in the peptide being distributed on both sides of the bilayer. As the passage of peptide through the pore is slow on the time scale of the simulations ( $>100$  ns), we do not achieve this state with the preformed bilayers.

**Pore Permeable to Lipids and Water.** Although peptide transport across the pore is too slow to be observed in the simulations, redistribution of lipids is observed. This is clearly evident in both Figures 2 and 4, where the headgroups of the lipids are colored according to which monolayer the lipid was in in the initial configuration. The number of flip-flops observed in the simulations ranges from one to five, with an average rate of two flip-flops per 100 ns. The flip-flops are always observed to take place from the peptide-enriched monolayer to the peptide-free monolayer. The number of water molecules that are able to permeate the pore is much larger. During the final 150 ns interval of a pore formed by four peptides under stress-free conditions (B4), unidirectional fluxes of 475 and 480 water molecules in each direction are observed. As expected in the absence of a driving force, the two unidirectional fluxes are of equal magnitude and do not lead to a net flux. The unidirectional flux  $J$  can be used to estimate the single-pore permeability coefficient  $P = J/C$ , where  $C = 55$  mol/L denotes the concentration of pure water. With  $J \approx 3$  waters/ns we obtain  $P \approx 1 \times 10^{-13}$  cm<sup>3</sup>/s. This is of the same magnitude as the single-channel permeability of aquaporin AQP4,<sup>42</sup> a channel with a relatively high permeation rate. As far as we know, no experimental measurements exist of single-pore permeability in the case of pores formed by antimicrobial peptides.

**Disordered Toroidal Pore Model.** Experimentally, it is also not possible to directly determine the number of peptides within the pore. The commonly cited number of  $\sim 4$ – $7$  peptides<sup>4,7</sup> has been indirectly inferred from a combination of neutron scattering data and oriented circular dichroism (OCD) measurements. The interpretation of these data is, however, dependent on two critical sets of assumptions. The first is that the pores are cylindrical. The second is that the peptides are helical and that all peptides involved in pore formation are oriented perpendicular to the plane of the membrane. In light of our simulations, these assumptions must be reconsidered. First, the pore is far from cylindrical. At the openings the pore is almost twice as wide as at the center. Second, the peptides are largely disordered and adopt a variety of orientations. The fact that the pores are not cylindrical could alter the estimate of the total area covered by the pores. The findings regarding the orientation of the peptide are, however, more significant. Currently, the available CD data are interpreted using a simple two-state (parallel/perpendicular) model. The fact that in the simulations the peptides stabilize the pore by binding close to the rim and do not necessarily adopt

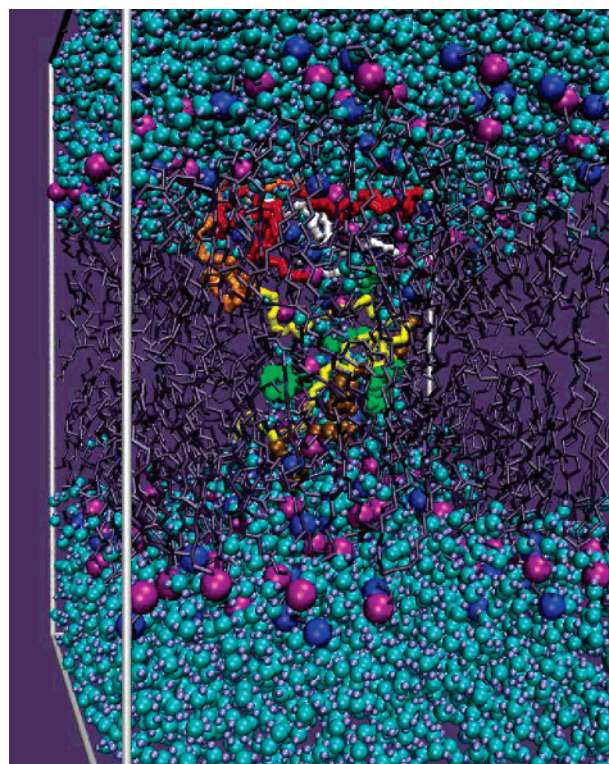


**Figure 5.** Disordered toroidal pore model. In the disordered toroidal pore model the peptides do not adopt a regular structure inside the pore, but rather maintain a diffuse distribution across the pore. The final structure ( $t = 250$  ns) of a spontaneously formed pore is shown. For the color code, see the other figure captions.

a fully perpendicular orientation has profound implications for interpretation of CD spectra and the estimation of the fraction of peptides involved in pore formation. In this regard we note that the irregular structure observed in the simulations is in fact in line with the conclusions drawn from recent NMR studies of magainin.<sup>40</sup> To capture the irregularity of the pore structure obtained from the simulations, we coin the term “disordered toroidal pore model” (DTP model), opposing the standard toroidal pore model. A representative snapshot illustrating this model is presented in Figure 5.

## Conclusions

The simulations in this work have for the first time allowed the elucidation of the mechanism by which a specific member of the magainin family of antimicrobial peptides, MG-H2, can induce a toroidal pore within a model phospholipid membrane. The significance of the work is that pore formation was observed to occur spontaneously and was not induced by artificial constraints. Notably, the structure of the pore that formed in the simulations while compatible with the available experimental data differs significantly from current idealized models of a toroidal pore. In particular, in the simulations the pore is stabilized by a diffuse distribution of peptides which bind to the rim of the pore, adopting a largely parallel orientation with respect to the plane of the membrane.

**Acknowledgment.** We thank Chris Chipot, Jesus Salgado, and Peter Tieleman for helpful discussions. This work was supported by the NWO Molecule-to-Cell program and by the Material Science Center (MSC+).

JA062927Q